



Author: Juodkazis, Kestutis; Juodkazyte, Jurga; Sebekas, Benjaminas; Savickaja, Irena; Juodkazis, Saulius
Title: Photoelectrochemistry of silicon in HF solution
Year: 2013
Journal: Journal of Solid State Electrochemistry
Volume: 17
Issue: 8
Pages: 2269-2276
URL: <http://hdl.handle.net/1959.3/316401>

Copyright: Copyright © Springer-Verlag Berlin Heidelberg 2013. The accepted manuscript is reproduced in accordance with the copyright policy of the publisher. The definitive version of the publication is available at www.springer.com.

This is the author's version of the work, posted here with the permission of the publisher for your personal use. No further distribution is permitted. You may also be able to access the published version from your library.

The definitive version is available at: <http://dx.doi.org/10.1007/s10008-013-2064-9>

Photoelectrochemistry of silicon in HF solution

Kęstutis Juodkazis · Jurga Juodkazytė ·
Benjaminas Šebeka · Irena Savickaja ·
Saulius Juodkazis

Received: date / Accepted: date

Abstract Photoelectrochemical, [photoelectrocatalytic](#) and electrochemical processes of silicon anodic oxidation and hydrogen evolution in aqueous HF solution are discussed in terms of thermodynamic stability of Si, oxides SiO, SiO₂ and Si surface hydrides. It is shown that photoelectrochemical oxidation of n-type low resistivity silicon to SiO₂ is catalyzed by Si⁺ photo-hole formation, whereas in the case of p-type Si, the feasibility of this reaction is predetermined by p-type conductivity. It is suggested that anodic oxidation of Si goes through the stage of SiO oxide formation and its subsequent oxidation to SiO₂. Such mechanism accounts for chemical inertness of Si phase in HF solutions as well as for selective, anisotropic and isotropic etching of Si within E ranges from -0.5 V to 0.35 V, 0.35-0.8 V, and $E > 0.8$ V, respectively. Hydrogen evolution reaction (HER) on Si surface proceeds at very large overpotential (≥ 0.5 V) through the stage of surface Si hydride formation: $\text{Si} + \text{H}_2\text{O} + \text{e}^- \rightarrow (\text{SiH})_{\text{surf}} + \text{OH}^-$ (the rate determining step) and $(\text{SiH})_{\text{surf}} + \text{H}_2\text{O} + \text{e}^- \rightarrow \text{Si} + \text{H}_2 + \text{OH}^-$. Illumination related effects of surface reactions relevant to selective and anisotropic etching and nano/micro-structuring of Si surface are discussed.

Keywords Methods of nanofabrication and processing · Nanostructured materials in electrochemistry · Semiconductor materials in electrochemistry · Thermodynamics of solutions · HER · electrodisolution of Si

PACS 81.16.-c · 82.45.Yz · 82.45.Vp · 82.60.Lf · 82.45.Qr

K. Juodkazis, J. Juodkazytė, B. Šebeka, I. Savickaja
Center for Physical Sciences and Technology, Institute of Chemistry, A. Goštauto 9, Vilnius
LT-01108, Lithuania

S. Juodkazis
Centre for Micro-Photonics, Faculty of Engineering and Industrial Sciences, Swinburne Uni-
versity of Technology, Hawthorn, VIC 3122, Australia
Melbourne Centre for Nanofabrication, 151 Wellington Road, Clayton, VIC 3168, Australia

1 Introduction

Silicon represents a chemical element which over past few decades has changed essentially the quality of our daily life. Invention of Si-based integral micro-chips was a revolutionary step in the production of various programmable devices and computers, which, in turn, promoted a major breakthrough in information and communication technologies and many other areas. So far, silicon is indispensable material for solar energy conversion into electricity. Above 90% of currently produced solar cells are silicon based [1]. However, this technology is quite expensive. Therefore intensive search for the ways to reduce the cost of solar electricity is very active field of research and engineering. Recently, porous silicon became quite attractive for solar-cell researchers, mainly because of its large surface area and low light reflection [2–4].

Physical, chemical and technological properties of silicon, its alloys and compounds have been thoroughly investigated and found applications in numerous technological processes [5,6]. The same can be said about its electrochemical and photoelectrochemical properties in aqueous solutions of various composition, which were comprehensively experimentally analyzed in relation to technologically very important silicon etching processes [7–16]. However, one has to admit that the nature and mechanisms of the photoelectrochemical processes taking place on Si electrode surface are not completely understood from the theoretical point of view so far [17], whereas these issues are of crucial importance in searching for effective energy conversion systems.

The main characteristic of electrochemical or photoelectrochemical process is voltammogram (VA), reflecting the dependence of the process rate on the electrode potential, i.e., the potential difference between electrode and solution phase. Because of semiconducting nature of silicon, the measurement of voltammetric characteristics and their analysis is quite problematic as Si electrodes can differ greatly one from another. Depending on the content of doping elements in silicon, which can vary between 10^{11} and 10^{20} atoms per cm^{-3} , the resistivity of Si ranges between 10^5 and 10^{-4} Ω cm, irrespective of the type of conductivity [18]. Therefore, when analyzing VAs, especially those of Si with high resistivity, it is necessary to take into account the value of ohmic potential drop within Si phase, which strongly depends on how the electric contact with Si was realized. **Moreover, when analyzing electrochemical behavior of Si, one has to take into consideration the fact, that two types of charge carriers, i.e. holes in valence band and electrons in conduction band can be involved in the electrochemical processes at the same time.**

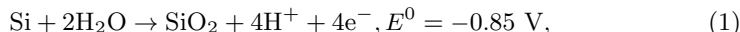
The present study was aimed at investigation of silicon anodic oxidation processes in the case of n- and p-type Si electrodes of low and high resistivity in aqueous HF solution. Effects of light illumination and their influence on the surface chemical changes are elucidated based on the thermodynamic properties of materials at the interface.

2 Theoretical background for analysis of experimental data

In order to understand the electrochemical behavior of silicon and the nature of the processes reflected in the voltammograms, it is worthwhile to analyze the sim-

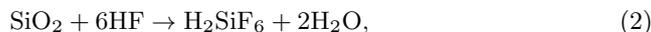
plified Pourbaix diagram for silicon presented in Fig. 1 [19]. It determines chemical stability limits and is reflecting the thermodynamical properties of the materials in contact. The dashed region depicts the employed experimental conditions in the case of 2 M HF solution. The dashed lines *a* and *b* denote the limits of thermodynamic stability of water. Water can be oxidized to O₂ (2H₂O - 4e⁻ → O₂ + 4H⁺) or reduced to H₂ (2H₂O + 2e⁻ → H₂ + 2OH⁻) at the potentials above and below lines *a* and *b*, respectively. Line *a* also reflects the pH-dependence of the potential of RHE electrode. Vertical dashed lines at pH = 10 and pH = 12 denote the equality between the concentrations of H₂SiO₃ and HSiO₃⁻ and also HSiO₃⁻ and SiO₃²⁻, respectively.

The main electrochemical process for silicon is described by the following reaction:



which is reflected by dependence (1) in the diagram (Fig. 1) and denotes the thermodynamic possibility of silicon anodic oxidation. Standard potential E^0 of this reaction ranges from -0.807 to -0.857 V for different crystalline modifications of SiO₂. pH-dependence for Eqn. 1 in Pourbaix diagram is situated below the line *b*, which means that silicon should evolve hydrogen from H₂O while oxidizing to SiO₂. It is well known [20] that Si reacts with water only in strongly alkaline medium, where SiO₂ dissolves yielding alkali-soluble silicates. It should be noted, however, that this reaction occurs at considerably more positive potentials, i.e. at $E \approx 0 \text{ V}$ (SHE) [27]. In acidic and neutral medium formation of insoluble SiO₂ layer on the surface of Si electrode should lead to blocking of the surface and passivation. It is noteworthy, however, that not the insulating layer of SiO₂ is the reason of silicon passivity and inactivity in acidic and neutral media.

In the solution of HF, native, thermal or anodically formed SiO₂ surface layer must be removed from Si surface due to following interaction [20]:



which produces a very stable complex [SiF₆]²⁻. Thus, the above reaction provides the possibility to investigate the anodic oxidation of Si phase in HF solution avoiding the complication of surface passivation. Skorupska et al. [21] have demonstrated that SiO₂ layer is completely removed from Si surface even in the dilute solution of NH₄F.

Another very important dependence in Fig. 1 is depicted by line 2. It represents the limit, which in accordance with thermodynamic data marks the transition between SiO₂ and gaseous silicon hydride SiH₄, in which oxidation degree of silicon is negative, i.e., takes value of $n_{\text{Si}} = -4$. Thus, it would follow, that the area between the lines 1 and 2 in Fig. 1 should represent the range of Si surface hydrides existence.

It is known from literature [12, 13] that after removal of surface oxide layer from Si with HF, the surface of silicon becomes covered with Si surface hydride ≡Si-H. In the review ref. [15] it has been demonstrated that silicon surface coverage with H atoms is about 10 at.%, whereas that of F atoms is below 0.1 at.%. Hence, if silicon surface coverage with H atoms is not continuous, it can hardly determine passivity of silicon in HF solutions [14, 16].

Moreover, SERS studies [22] showed that in addition to Si-H bonds, Si-O and Si-OH ones are also formed on the the surface of silicon during anisotropic etching

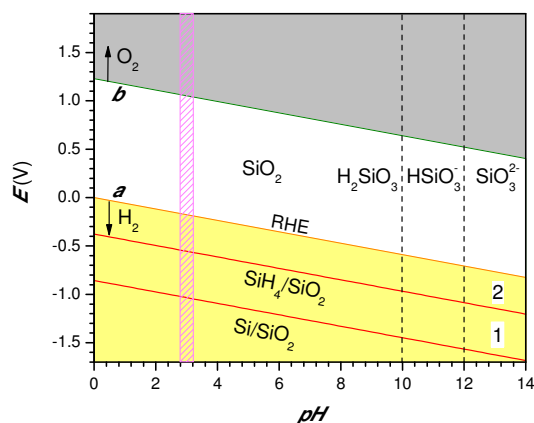


Fig. 1 The simplified Pourbaix diagram for silicon. The dash-boxed region indicates conditions of experiments.

in 0.05 M fluoride medium (pH 3) within 0 - 0.6 V (vs. Ag/AgCl). It has been also demonstrated that at $E \approx -0.3$ V, i.e., in the vicinity of open-circuit potential (OCP), the surface of silicon is clean from the above indicated species. Houbertz et al. [23] showed that while the surface of Si electrode is free from oxides in the cathodic range of potentials, i.e., at $E < E_{\text{OCP}} \approx -0.97$ V (Ag/AgCl in 40% NH_4F , pH 8), a thin layer of oxides (1.0 - 1.5 mono-layer) is already present on the surface within the double layer region, whereas in the range of anisotropic anodic etching ($E > 0$ V (Ag/AgCl)) the amount of oxygen on Si surface increases several times.

Thus the above described data show that anodic oxidation of Si proceeds via formation of silicon oxygen species on the electrode surface, i.e. that reaction goes via oxide- rather than fluoride-route [14,16]. Interaction of Si phase with H_2O is much more fundamental compared to interaction of silicon with HF molecules, because Si-O chemical bond is much stronger than Si-F (800 kJ mol^{-1} and 540 kJ mol^{-1} [24], respectively). The results obtained in the present study fully support this point of view.

3 Experimental

The working n- and p-type Si electrodes were prepared by mechanically cutting 5×20 mm plates from 100×0.5 mm silicon discs (Nilaco) of low resistivity Si ($< 0.02 \Omega \text{ cm}$). In order to realize an ohmic contact with Si phase, immersion gold coating was deposited on the whole surface of Si plates except for 5×10 mm working area, which was isolated by covering with chemically resistant poly-vinylchloride lacquer. After that immersion gold coating was electroplated with pure gold coating to obtain thickness of $\sim 0.1 \mu\text{m}$. Then isolating layer of lacquer was removed from working Si electrode surface and applied to gold surface, which was exposed to electrolyte. Thus, the electric contact was realized just 0.5 mm or by the plate thickness away from the working Si surface. Taking into account low resistivity of silicon and gold coating as well as a small distance (1 to 2 mm) between the

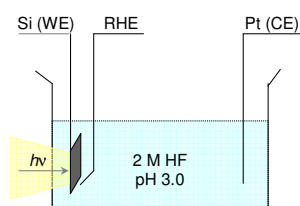


Fig. 2 Schematics of electrochemical cell for photoelectrochemical measurements. WE - working electrode, CE - counter electrode, RHE - reference hydrogen electrode. Electrical circuit was completed by a potentiogalvanostat.

working Si surface and the end of Luggin capillary, the overall ohmic potential drop during voltammetric measurements did not exceed 5 to 10 mV at current densities up to 10 mA cm^{-2} . Voltammetric investigations were performed using a potentiogalvanostat PGSTAT302 (Autolab, Eco Chemie), plastic cell with 50 cm^3 volume, Pt wire as counter electrode and reference hydrogen electrode (RHE) adjusted for measurements in HF solutions. Potential values in the text and figures refer to the standard hydrogen electrode (SHE) unless noted otherwise. The electrolyte was a 2 M aqueous solution of hydrofluoric acid ($\text{pH} \approx 3$). Analytical grade HF and deionized water were used to prepare the solutions. Schematic representation of the cell is shown in Fig. 2.

For the measurement of voltammetric response of Si electrode in dark the cell was placed into Faraday cage and light proof enclosure. Photoactivation was qualitatively tested using illumination by a standard 100 W incandescent lamp without focusing.

The rate of corrosion of n- and p-type Si in 2 M HF was determined by means of measuring the decrease in weight of specimens after 260 h exposure to 2 M HF solution in dark and under [natural illumination, which included alternation of day and night](#) (“in light”). All experiments were carried out at room temperature (20 – 25 °C). The specimens were placed into transparent and opaque plastic containers, which were filled to the capacity with electrolyte. The weight of the specimens was measured using analytical weights GR-202 (A&D Company, Ltd. Japan).

4 Results: Photo-electrochemical processes of low & high resistivity Silicon

Variation of the open-circuit potential $E_{i=0}$ of highly doped n-Si and p-Si electrodes in the solution of 2 M HF ($\text{pH} 3$) under illumination is shown in Fig. 3. One can see that initially $E_{i=0}$ values of p-Si and n-Si electrodes in dark are -0.6 V and -0.35 V, respectively. This shows that p-Si is significantly more active than n-Si, from the electrochemical point of view. The shift of the open-circuit potential under illumination, i.e., $\Delta E_{\text{ph}} = E_{i=0}^{\text{light}} - E_{i=0}^{\text{dark}}$ is negative for n-Si and positive for p-Si. In the case of n-Si, negative shift of $E_{i=0}$ upon illumination (Fig. 3) is determined by facilitation of anodic process, while for p-Si cathodic process becomes more facile and $E_{i=0}$ shifts positively. In time, open-circuit potentials of both electrodes approach the stationary value of -0.5 V, which corresponds to the beginning of hydrogen evolution on Si surface, as will be shown further.

Cyclic voltammograms of highly doped low resistivity n- and p-type silicon in 2 M HF solution in dark and under illumination conditions are presented in

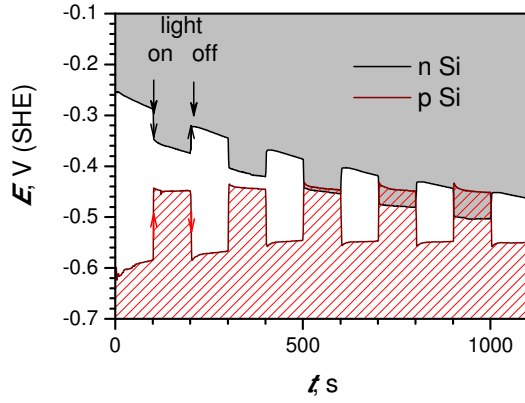


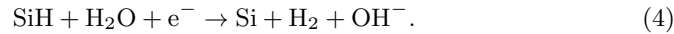
Fig. 3 Variation of open-circuit potential of n- and p-type low resistivity ($< 0.02 \Omega \text{ cm}$) silicon in 2 M HF (pH 3) under illumination, 20°C .

Fig. 4. The positively proceeding part of the VA is always below the negative one for the n-type Si under illumination and for p-type Si in both dark and under light. Moreover, in the case of multiple cycling (10 - 20 cycles), the last VA is always shifted negatively compared to the first one. From the electrochemical point of view, such facilitation should be related with activation of Si electrode, i.e., with an increase in electrochemically active surface area.

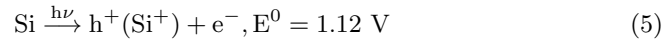
Figure 4a shows summary view of all voltammetric investigations within range of moderate ($\leq 10 \text{ mA cm}^{-2}$) current densities. As one can see from Fig. 4a, voltammograms of n- and p-type silicon under illumination are very similar in both cathodic and anodic regions. There is no doubt that overall anodic process involves oxidation of Si to SiO_2 and removal of this oxide in form of $[\text{SiF}_6]^{2-}$ complex, as a consequence of interaction with HF, whereas cathodic process is hydrogen evolution [21,25], which should go through the stage of Si surface hydride (chemisorbed H atom) formation, the rate determining step:



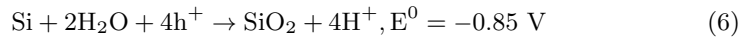
and subsequent fast step of H_2 electrochemical desorption:



As one can see from VAs presented in Fig. 4a, anodic oxidation of n-Si in light is facile and proceeds at a considerable rate, whereas in dark the beginning of the process is shifted by $\sim 500 \text{ mV}$ towards more positive potentials and the rate is significantly lower. Thus it is evident that the process is accelerated by Si holes, i.e. Si^+ ions photo-generated in valence band. Overall process of photoelectrochemical oxidation of Si can be described by the following reactions:



and



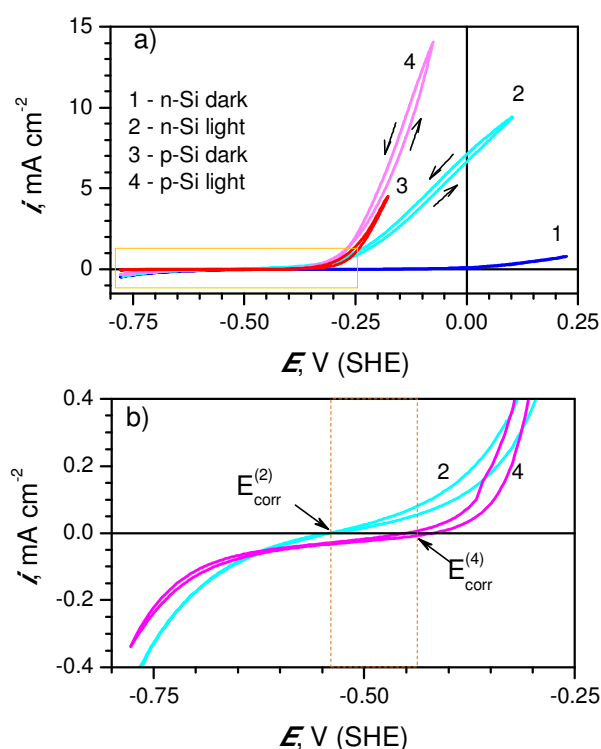


Fig. 4 (a) Cyclic voltammograms of n- and p-type low resistivity ($< 0.02 \Omega \text{ cm}$) silicon in 2 M HF (pH 3) in dark and under illumination; $v = 20 \text{ mV s}^{-1}$, 20°C . (b) Close up view of the box-marked region in (a).

The value of standard potential of eq. 6 is the same as that of eq. 1, because the thermodynamics of the process does not depend on the reaction route. It follows from the eq. 6, that photo-electrochemical oxidation of Si should be independent of whether Si^+ holes were photogenerated, or have originated from dopant elements (e.g., B or Mg) yielding p-type conductivity. This is experimentally confirmed by VAs of p-type Si shown in Fig. 4a, where one can see that in the case of sufficiently high conductivity and corresponding intensity of illumination, the rates of Si anodic oxidation in light and in dark are very similar.

Figure 4b shows more detailed view of VAs of n- and p-type Si in light in the range of small current densities ($\leq 1 \text{ mA cm}^{-2}$). As one can see from Fig. 4b, at $i = 0$ potentials $E_{\text{corr}}^{(2)}$ and $E_{\text{corr}}^{(4)}$ mark the points, where the rates of both above described anodic and cathodic processes are equal for n-Si and p-Si in light, respectively. In other words, at $i = 0$ photochemical corrosion of Si proceeding with hydrogen depolarization can take place. Comparison of average value of $E_{\text{corr}}^{(2)}$ and $E_{\text{corr}}^{(4)}$, i.e. $\sim -0.5 \text{ V (SHE)}$, with standard potentials of the above mentioned anodic and cathodic processes, i.e., $E_{\text{SiO}_2/\text{Si}}^0 = -0.85 \text{ V (SHE)}$ and $E_{2\text{H}^+/\text{H}_2}^0 = 0 \text{ V (SHE)}$, reveals that both the anodic oxidation of Si and evolution of H_2 proceed at relatively large overpotential, i.e., $\sim 0.35 \text{ V}$ and -0.50 V , respectively.

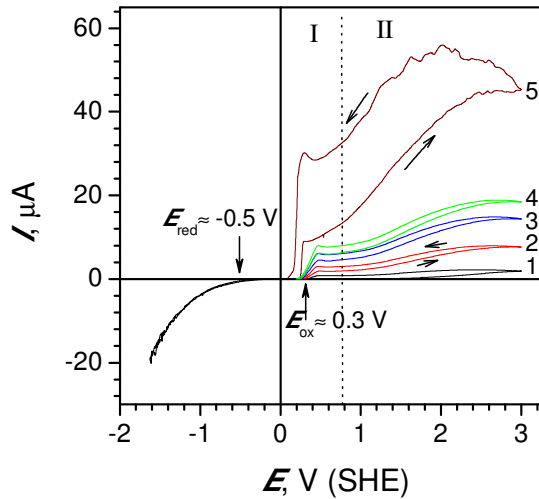


Fig. 5 Cyclic voltammograms of high resistivity ($> 10^3 \Omega\text{cm}$) n-type Si(100) electrode in 2 M HF (pH 3): 1-4 – consecutive cycles recorded without illumination, 5 – with back-side illumination, $v = 20 \text{ mV s}^{-1}$, 20°C ; data taken from ref. [17]. Potential regions I and II denote anisotropic (porous Si) and isotropic etching conditions, respectively.

The overall rate of photochemical and chemical corrosion of p-Si and n-Si in light and in dark evaluated from the decrease in mass of Si specimens exposed to HF solution is presented in Table 1. As one can see, the rate of Si chemical and photochemical corrosion in the solution of 2 M HF (pH 3) is rather small. When converted into current density units, it ranges between 1 and $2 \mu\text{A cm}^{-2}$. Only in the case of p-Si in light the rate of corrosion as high as $\sim 6 \mu\text{A cm}^{-2}$ was determined. The rate of purely chemical corrosion proceeding with hydrogen depolarization is $\sim 0.7 \mu\text{A cm}^{-2}$ and $\sim 1.4 \mu\text{A cm}^{-2}$ as was obtained for the case of n-Si and p-Si in dark, respectively. Thus the above mentioned passivity of silicon in acid and neutral solutions should be determined by the low rate of chemical corrosion of Si due to high overvoltage of H_2 evolution. Besides, the oxidation of Si itself according to eq. 6 should be slow complex stepwise process.

As it has already been mentioned above, from the comparison of VAs of n-Si in dark and in light (Fig. 4a) it follows that in deficiency of holes, i.e., Si^+ ions on the electrode surface, irrespective of whether they originate from alloying elements or as a result of illumination, branch of voltammogram, reflecting the process of Si anodic oxidation, shifts towards more positive E values, whereas more appreciable rate of anodic oxidation is observed only at $E > 0 \text{ V (SHE)}$ (Fig. 4a).

Regarding an onset potential of the Si anodic oxidation, it is interesting to compare the experimental data (Fig. 4) with literature, which usually refer to lowly doped high resistivity Si electrodes. In ref. [7], summarizing the electrochemical behavior of p- and n-type Si electrodes in the range of high current densities ($\sim 200 \text{ mA cm}^{-2}$) and high voltages ($\pm 8.0 \text{ V}$), it was indicated that the boundary between cathodic and anodic processes is at $E \approx 0 \text{ V}$. The same value of boundary potential in the fluoride-free solution of 2 M KOH was reported in ref. [27]. In a precise study by Outemzabet et al. [22], where surface state of Si in 0.05 M HF (pH 1.0 - 3.0) was studied using FTIR spectroscopy, it was demonstrated that

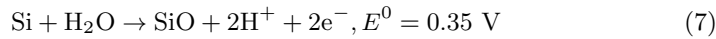
Table 1 Rates of chemical and photochemical corrosion ($i=0$) of low-resistivity n- and p-type silicon during 260 h exposure to 2 M HF (pH 3), 20 – 25°C

Sample (illumination)	Δm [mg]	Corrosion rate [mg cm ⁻²]	Corrosion rate [$\mu\text{A cm}^{-2}$]
n-Si (in light)	-0.14	-0.097	1.4
n-Si (in dark)	-0.09	-0.055	0.7
p-Si (in light)	-0.32	-0.463	6.4
p-Si (in dark)	-0.09	-0.100	1.4

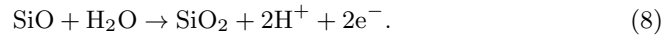
anodic oxidation of Si begins at $E \approx 0.4$ V (SHE) irrespective of crystallographic orientation of Si surface. In our previous study [17] the beginning of anodic oxidation of lowly doped ($\rho = 1000 \Omega \text{ cm}$) n-type Si in 2 M HF (pH 3) was observed at 0.2 - 0.3 V (SHE) (Fig. 5), whereas the onset of H₂ evolution - at $E \approx -0.5$ V (SHE), similarly to highly-doped Si (Fig. 4a). In the case of such layout of anodic and cathodic processes, corrosion of Si with hydrogen depolarization becomes absolutely impossible at $E > -0.5$ V. Thus, in the case of lowly doped n-Si, the E range between -0.5 V and ~ 0.3 V (SHE) (Fig.5) represents the region of Si phase immunity, which is referred to as double layer region in literature [23].

The E range of high resistivity n-Si anodic oxidation can be divided into two regions as shown in Fig. 5. It is known from literature that these regions correspond to ranges of anisotropic and isotropic Si etching, respectively [7–11,28]. In the first region, beginning at 0.2 - 0.3 V (SHE) rather sudden increase in anodic current is observed, whereas in the second one, beginning at $E > 0.8$ V, second current wave can be discerned. The rate of anodic process within 2nd E range increases relatively very slowly. A back-side illumination of Si considerably increases the rate of anodic process in both regions [17]. It is interesting to note that similar sharp increase in current density at $E \approx 0.4$ V (SHE) was observed in ref. [22] for various crystallographic Si planes in 0.05 M HF solution at pH = 1 and pH = 3.

Thus it is evident that anodic oxidation of lowly-doped high resistivity silicon to SiO₂ proceeds at significantly larger overpotential ($\eta \approx 0.3 - (-0.85) = 1.15$ V) as compared to highly-doped low resistivity Si (Fig. 4), where η is just ~ 0.35 V ($-0.50 - (-0.85) = 0.35$ V). It is reasonable to presume that electrochemical oxidation of Si to SiO₂ according to eq.1 proceeds stepwise, i.e., first E range from ~ 0.3 V to ~ 0.8 V (SHE) corresponds to formation of Si(II) oxide - SiO, whereas second one at $E \geq 0.8$ V - to formation of Si(IV) oxide SiO₂, as described by following reactions:



and



The value of standard potential of eq. 7, $E_{\text{SiO/Si}}^0 = 0.35$ V was calculated from the thermodynamic data for SiO given in ref. [29], i.e., $\Delta H^0 = -103 \text{ kJ mol}^{-1}$, $\Delta S^0 = 211 \text{ J mol}^{-1} \text{ K}^{-1}$ and $\Delta G^0 = -160 \text{ kJ mol}^{-1}$. It is noteworthy, that E^0 of eq. 7 coincides almost precisely with the beginning of electrochemical anodic oxidation of lowly doped high resistivity n-Si, which is observed at $E \approx 0.3$ V (SHE)(Fig. 5).

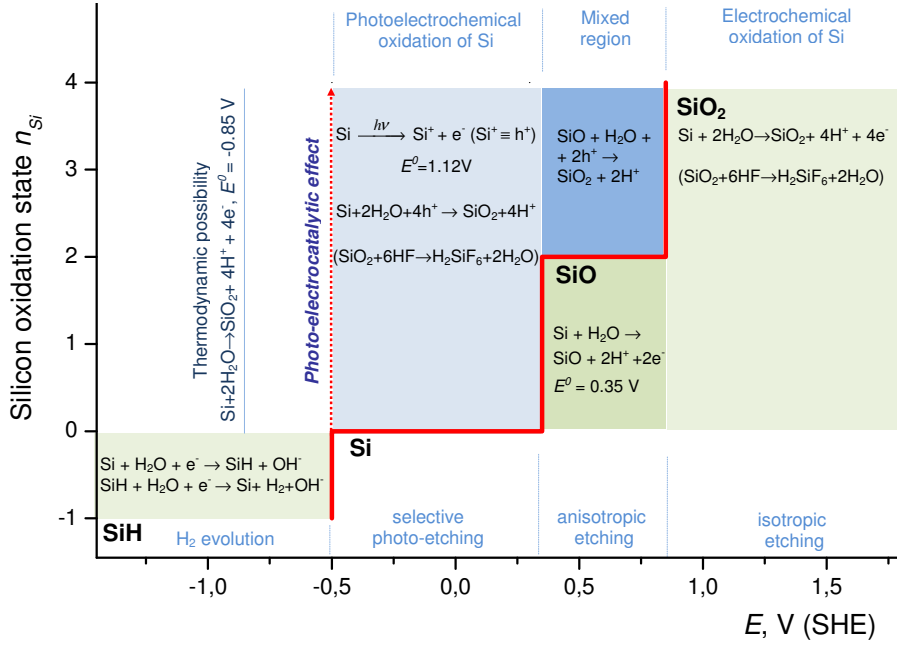


Fig. 6 Summary of the (photo-)electrochemical processes of Si in aqueous HF solutions. The vertical arrow shows a change of oxidation state of Si upon absorption of photons with energy $h\nu > E_g$ ($E_g = 1.12$ eV [26]); broken line separates the regions of photoelectrochemical and electrochemical oxidation of Si, see text for details.

5 Discussion

Summary view of the photoelectrochemical and electrochemical processes taking place on high and low resistivity silicon in 2 M HF, pH 3 at 20 °C is presented in Fig. 6. Main possible reactions of Si oxidation and H_2 evolution are written in specific E regions separated by dashed lines. As shown in Fig. 6, photoelectrochemical or photo-electrocatalytic oxidation of Si is possible within a wide range of potentials, i.e. from ~ -0.5 V to ~ 0.35 V (SHE). Naturally, such process cannot proceed in the absence of holes (eq. 5), i.e. in dark at low n-type conductivity of Si phase. Therefore the range between ~ -0.5 V and ~ 0.35 V is called the zone of immunity (stability) of Si phase or double layer region [23]. This zone separates the regions of oxide and hydride species formation or the regions of positive and negative oxidation state of Si.

Actually, electrochemical oxidation of Si begins at $E \approx 0.3$ V (SHE) (see Fig.5). The overvoltage for this process is as large as ~ 1.15 V, which is tantamount to the width of silicon band gap E_g . As suggested above, photoelectrochemical and electrochemical oxidation of Si most likely proceeds through an intermediate stage of Si(II) oxide SiO formation, because, attachment of two O^{2-} ions from H_2O molecules by one Si atom in atomic plane is impossible from the steric point of view, as radii of Si atom and O^{2-} ion are almost equal, i.e., 0.268 nm and 0.272 nm, respectively [30]. Moreover, E range between ~ 0.35 V and ~ 0.8 V (SHE) is known to be the region of anisotropic etching of Si, where macro pores with diameter

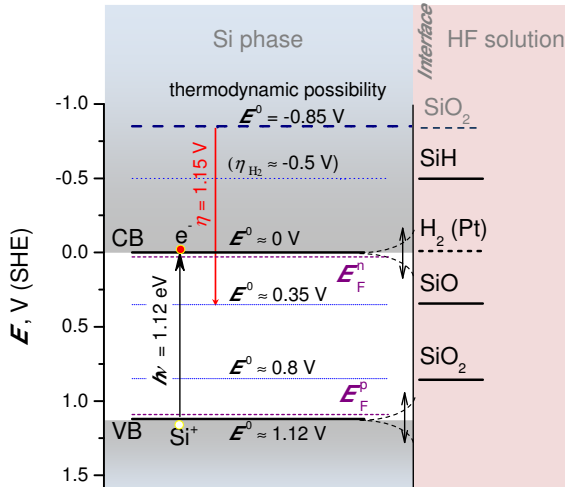
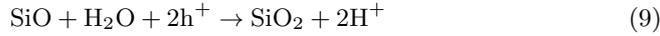


Fig. 7 Energy diagram for Si surface photo-electrochemical reactions. Optical electron-hole excitation in Si phase is equivalent to the electrochemical potential change by +1.12 V; potentials of actual oxidation of Si and reduction of H₂ are shown. The $E_{F}^{n,p}$ are the Fermi levels for electrons (n) and holes (p), respectively; their position and actual band bending upon contact with electrolyte (HF) will depend on the doping, applied voltage and photo-excitation. The η_{H_2} is the overpotential of H₂ evolution on Si. CB and VB - conduction and valence bands.

of several microns and aspect ratio exceeding 120 can be formed [28]. Selective anisotropic photoelectrochemical etching of Si within E range between ~ 0.35 V and ~ 0.8 V can be explained by sequence of reactions 7 and photoelectrochemical oxidation of SiO to SiO₂ as described by:



Due to the sequence of reactions (7) and (9), it is possible to control the rate of anodic oxidation of Si with the help of potential E and back-side illumination and perform selective anisotropic etching of silicon [7,9–11]. Selective photo-etching **under front-side illumination** is possible within E range from -0.5 V to 0.35 V, as can be seen from comparison of VAs recorded in light and in dark for n-Si in Fig. 4a.

At $E > 0.8$ V (SHE) Si atoms, as well as SiO oxide, can be directly electrochemically oxidized to SiO₂ state, which is the reason why selective anisotropic etching turns to isotropic, i.e. uniform in all directions. As one can see from Fig. 6, there is a clear demarcation line between the ranges of photoelectrochemical and electrochemical oxidation of Si.

Fig. 7 shows potential levels representing oxidation/reduction processes of Si phase. It is well-known that in the case of metals, valence band (VB) and conduction band (CB) levels coincide. Shift of this level towards anodic or cathodic potentials determines what reaction will take place on the electrode surface. In the case of semiconductors, valence band and conduction band levels are separated by a forbidden energy band of width E_g . Positive charge carriers, i.e. holes in VB can participate in anodic oxidation reactions, whereas electrons in CB can take part in cathodic reduction processes. As one can see from the layout of silicon conduction

and valence bands, illumination or doping produced Si^+ holes have sufficiently high potential to oxidize Si surface atoms to SiO or SiO_2 oxides according to eq. 6, i.e. photoelectrochemically (Fig. 7). The conduction band level of Si phase is determined by the value of chemical potential of Si, i.e. $\mu^0 = 0$ cal [19]. Therefore, Si^+ hole represents strong oxidizer ($E_{\text{Si}^+/\text{Si}}^0 = 1.12$ V) with oxidative energy almost tantamount to that of oxygen ($E_{\text{O}_2/\text{H}_2\text{O}}^0 = 1.23$ V), whereas Si oxidation to SiO_2 is thermodynamically possible at $E_{\text{SiO}_2/\text{Si}}^0 = -0.85$ V. As one can see from Fig. 4b, the equilibrium between anodic and cathodic processes in the case of Si samples investigated settles at $E = -0.5 \pm 0.05$ V, i.e. at the beginning of H_2 evolution on Si surface. Corrosive nature of $E_{i=0}$ explains simultaneous existence of Si=O and Si-H compounds and $\text{Si}^+ \cdot \text{OH}^-$ ionic pair on the electrode surface, what was demonstrated experimentally in refs. [22, 23].

As a result of anodic polarization of Si electrode, CB level can reach the potential of 0.3 V or even 0.8 V. This would increase the oxidative power of Si^+ holes, however, direct electrochemical oxidation of Si atoms to SiO or SiO_2 will also become possible, as shown in Figs. 6 and 7.

From the above presented analysis it follows that use of Si photoelectrode as anode in electrochemical solar cells in HF solutions would inevitably lead to its anodic dissolution. If such photoanode was connected with Pt electrode and used for production of solar hydrogen in HF solution, the process would proceed until complete dissolution of Si phase. Therefore, the process of irreversible anodic oxidation of Si to SiO_2 should be avoided or eliminated in a photoelectrochemical systems intended for effective solar energy conversion. Processes on the surfaces of photo-electrodes [31] are critically important for the development of next generation of solar cells, photo-anodes and for laser nano-micro structuring of surfaces via laser-induced wet etching including front- and backside illumination which has found number of applications in lab-on-a-chip.

6 Conclusions

Summary of the conclusions discussed and analyzed here is the following:

- Anodic oxidation of Si to SiO_2 in HF solution can proceed either photoelectrochemically, i.e. with participation of holes of valence band, or electrochemically, i.e. with participation of electrons of conduction band.
- Both photoelectrochemical and electrochemical oxidation of Si go through intermediate stage of SiO oxide formation.
- Photoelectrochemical or, in other words, photoelectrocatalytic oxidation of Si is more facile, i.e. it proceeds at lower overpotential ($\eta \approx 0.35$ V) than electrochemical one ($\eta \approx 1.15$ V).
- From the energetic point of view, energy required for photoactivation of Si, i.e. ~ 1.12 eV, is tantamount to electrochemical one, i.e. ≈ 1.15 eV.
- Photoelectrochemical corrosion of Si in HF solution proceeds with hydrogen depolarization.

New insights into photo-electrochemical processes discussed here are relevant to corrosion and longevity issues of silicon-based photovoltaic devices.

Acknowledgements SJ is grateful for support via VP1-3.1-ŠMM-01-V-02-001 grant.

References

1. Asim N, Sopian K, Ahmadi S, Saeedfar K, Alghoul MA, Saadatian O, Zaidi SH (2012) A review on the role of materials science in solar cells. *Ren Sustain Energy Rev* 16:5834–5847
2. Kopitkovas G, Mikulskas I, Grigoros K, Šimkienė I, Tomašiūnas (2001) Solar cells with porous silicon: modification of surface-recombination velocity. *Appl Phys A* 73:495–501
3. Badawy WA (2008) Effect of porous silicon layer on the performance of si/oxide photovoltaic and photoelectrochemical cells. *J Al. Comp* 464:347–351
4. Lewerenz H, Aggour M, Stempel T, Lublow M, Grzanna J, Skorupska K (2008) Photoactive nanostructure device by electrochemical processing of silicon. *J Electroanal Chem* 619-620:137–142
5. Crabtree GW, Lewis NS (2007) Solar energy conversion. *Physics Today* 60:37–42
6. Razykov T, Ferekides C, Morel D, Stefanakos E, Ullal H, Upadhyaya H (2011) Solar photovoltaic electricity: Current status and future prospects. *Solar Energy* 85:1580–1608
7. Lehmann V (1996) Porous silicon formation and other photoelectrochemical effects at silicon electrodes anodized in hydrofluoric acid. *Appl Surf Sci* 106:402–405
8. Jakubowicz J (2007) Nanoporous silicon fabricated at different illumination and electrochemical conditions. *Superlattices and Microstructures* 41:205–215
9. Lehman V, Föll H (1990) Formation mechanism and properties of electrochemically etched trenches in n-type silicon. *J Electrochem Soc* 137:653 - 659
10. Lehman V (1993) The physics of macropore formation in low doped n-type silicon. *J Electrochem Soc* 140:2836 - 2843
11. Lehman V, Grüning U (1997) The limits of macropore array fabrication. *Thin Solid Films* 297:13-17
12. Ubara H, Imura T, Hiraki A (1984) Formation of Si-H bonds on the surface of microcrystalline silicon covered with SiO_x by HF treatment. *Sol State Commun* 50:673–675
13. Burrows VA, Chabal YJ, Higashi GS, Raghavachari K, Christman SB (1988) Infrared spectroscopy of Si(111) surfaces after hf treatment: Hydrogen termination and surface morphology. *Appl Phys Lett* 53:998–1000
14. Gerisher H, Allongue P, Kieling VC (1993) The Mechanism of the anodic oxidation of silicon in acidic solutions Fluoride Solutions revisited. *Ber Bunsenges Phys Chem* 97:753–756
15. Smith RL, Collins SD (1992) Porous silicon formation mechanisms. *J Appl Phys* 71:R1–R22
16. Kolasinski KW (2003) The mechanism of Si etching in fluoride solutions. *Phys Chem Chem Phys* 5:1270–1278
17. Juodkazis K, Juodkazytė J, Kalinauskas P, Gertus T, Jelmakas E, Misawa H, Juodkazis S (2010) Influence of laser microfabrication on silicon electrochemical behavior in hf solution *J Sol State Electrochem* 14:797–802
18. Koshkin NI, Shirkevich MG (1980) *Spravochnik po elementarnoy fizike*. Nauka, Moscow
19. Pourbaix M (1963) *Atlas d'équilibres électrochimiques*. Gauthier-Villars, Paris
20. Akhmetov N (1981) *Obshchaya i neorganicheskaya khimiya*. Vyshaya Shkola, Moscow (in Russ.)
21. Skorupska K, Lublow M, Kanis M, Jungblut H, Lewerenz HJ (2005) On the surface chemistry of silicon under reducing conditions: an SRPES investigation. *Electrochem Comm* 7:1077-1081
22. Outemzabet R, Cherkaoui M, Gabouze N, Ozanam F, Kesri N, Chazalviel J-N (2006) Origin of the anisotropy in the anodic dissolution of silicon. *J Electrochem Soc* 153:C108–C116
23. Houbertz R, Memmert U, Behm RJ (1998) On the potential-dependent etching of Si(111) in aqueous NH₄ solution. *Surf Sci* 369:198-211
24. Rabinovich VA, Khavin ZY (1977) *Kratkiy khimicheskiy spravochnik*, Khimiya, Leningrad.
25. Kimura Y, Nemoto J, Niwano M (2002) Electrochemistry on Si(100) in a hydrofluoric acid solution at cathodic potential regions. *Mat Sci Eng B* 96:107-110
26. K. W. Böer (1990) *Survey of semiconductor physics: electrons and other particles in bulk semiconductors*. vol. I, Van Nostrand Reinhold, New York
27. Chen L-C, Chen M, Wan CC, Tsaur TH, Lien C (1995) Selective etching of silicon in aqueous KOH. *Mater Sci Eng B* 34:180–187
28. Klür MH, Sauer mann A, Elsner CA, Thein KH, Dertinger SK (2006) Partially oxidized macroporous silicon: a three-dimensional photonic matrix for microarray applications. *Adv Mat* 18:3135–3139

-
29. Karapetjanc MK, Karapetjanc ML (1968) Osnovniye termodinamicheskiye konstanty neorganicheskikh i organicheskikh veshchestv. Khimiya, Moscow
 30. Emsley J (1991) The Elements. Oxford, Clarendon Press
 31. Juodkasis K, Juodkazytė J, Kalinauskas P, Jelmakas E, Juodkasis S (2010) Photoelectrolysis of water: Solar hydrogen - achievements and perspectives. Opt Express: energy express 18:A147–A160